Revista Brasileira de Ciências Ambientais
Brazilian Journal of Environmental Sciences

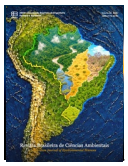

Remote sensing applied to biophysical parameters and land cover to identify urban heat islands in Recife (PE), Brazil

Sensoriamento remoto aplicado em parâmetros biofísicos e cobertura do solo para identificação de ilhas de calor urbana em Recife (PE), Brasil

Haylla Rebeka de Albuquerque Lins Leonardo[1], *Debora Natália Oliveira de Almeida*[1], *Alessandro Rodrigues de Amorim*[1], *Anderson Luiz Ribeiro de Paiva*[1], *Leidjane Maria Maciel de Oliveira*[1], *Sylvana Melo dos Santos*[1]

ABSTRACT

Urban growth results in several changes, mainly related to demographic, social, economic, and environmental aspects, leading to a new connotation in the use and occupation of land. This new scenario impacts the local energy balance, creating what is called an "urban heat island". This study aims to investigate the occurrence of urban heat islands in Recife city, the capital of Pernambuco, Brazil, based on the processing of biophysical parameters, the classification of land use and occupation, and surface temperature. The orbital images of the study region were obtained and processed using the Google Earth Engine cloud processing platform from 2013 to 2021. The results showed an increase in areas with greater urban density and a reduction in areas with vegetation. It was realized that in regions with greater urban density, the surface temperature observed was up to 5.20°C higher than in the area with vegetation.

Keywords: Built-Up Index; biophysical indexes; Google Earth Engine.

RESUMO

Do crescimento urbanístico resultam diversas alterações relacionadas, principalmente, com aspectos demográficos, sociais, econômicos e ambientais, decorrendo em uma nova conotação no uso e ocupação do solo. Esse novo cenário impacta o balanço energético local, gerando, como é conhecida, uma "ilha de calor urbana". Esta pesquisa objetiva investigar a ocorrência de ilhas de calor urbana na cidade do Recife, capital de Pernambuco, Brasil, a partir do processamento de parâmetros biofísicos, da classificação do uso e ocupação do solo e da temperatura da superfície. As imagens orbitais da região de estudo foram obtidas e processadas utilizando-se a plataforma de processamento em nuvem Google Earth Engine, para o período de 2013 a 2021. Os resultados evidenciaram a ocorrência de um aumento das áreas com maior densidade urbana e uma redução das áreas com vegetação. Constatou-se que nas regiões com maior densidade urbana, a temperatura de superfície observada foi até 5,20°C mais elevada do que na área com vegetação.

Palavras-chave: *Built-Up Index*; índices biofísicos; *Google Earth Engine.*

[1]Federal University of Pernambuco – Recife (PE), Brazil.

Corresponding author: Haylla Rebeka de Albuquerque Lins Leonardo – Federal University of Pernambuco – Avenida da Arquitetura, s/n – Cidade Universitária – CEP: 50740-550 – Recife (PE), Brazil. E-mail: haylla.rebeka@ufpe.br

Conflicts of interest: the authors declare no conflicts of interest.

Funding: doctoral scholarship with number IBPG-1657-3.01/21 by Foundation for the Support of Science and Technology of Pernambuco (FACEPE — *Fundação de Apoio a Ciência e Tecnologia do Estado de Pernambuco*) for the first author; doctoral scholarship with number process number 88887.827976/2023-00 by Coordination for the Improvement of Higher Education Personnel (CAPES — *Coordenação de Aperfeiçoamento de Pessoal de Nível Superior*) for the second author; research project with process number 408269/2023-5 and title "Use of socio-inclusive green technologies as measures for urban drainage control" by The National Council for Scientific and Technological Development (CNPQ — *Conselho Nacional de Desenvolvimento Científico e Tecnológico*) for the last author.

Received on: 05/06/2024. Accepted on: 09/01/2024.

https://doi.org/10.5327/Z2176-94782107

This is an open access article distributed under the terms of the Creative Commons license.

Introduction

Urbanization is an anthropogenic alteration that generates changes in surface materials due to vegetation suppression, albedo variation, and soil impermeabilization, influencing the local energy balance (Almeida et al., 2021). According to Borges et al. (2022), artificial surface covers significantly modify the radiation components of energy balance and near-surface wind, contributing to the formation of urban heat islands (UHI).

Studies by Cheela et al. (2021) and Yin et al. (2023) stated that the characteristics of cities' spatial configuration, the different types of land use such as darker surfaces, vegetation, and water distribution, as well as the absorption of long-wave radiation in peri-urban areas, and the significant increase in the temperature difference of the underlying surface contribute to the formation of the heat island effect.

Research on UHI has gained popularity in recent decades due to the growing recognition of thermal stress impacts on human health, environments, and urban resilience. The development of remote sensing technology has been widely applied to UHI research to understand its spatiotemporal characteristics better (Diem et al., 2024).

Using orbital data, it is possible to process land surface temperature (LST), which provides a thermal perception of the Earth's surface depending on land use/cover categories. According to Bagyaraj et al. (2023), the mathematical formulation of LST takes into account the physical process of surface energy to provide information on temporal variations. It serves as an indicator for monitoring vegetation as well as climatic and construction-related changes.

Increasing LST is an early indicator of potential risks and helps understand climate change. Therefore, the subject is current, and several studies have already reported on LST (Imran et al., 2019; Almeida et al., 2021; Moazzam et al., 2022; Venkatraman et al., 2024).

However, UHI studies' limitations include dependence on static datasets, neglect of microscale variations, and potential oversimplification of complex urban dynamics. These limitations can hinder accurate assessments of heat island effects, impacting the development of effective mitigation strategies for urban areas, as Venkatraman et al. (2024) highlighted.

To address these limitations, Ward et al. (2016) emphasized that remote sensing techniques can create spatially explicit UHI maps and models, allowing the detection of sensitive urban areas and the application of focused mitigation and adaptation strategies.

According to Peng et al. (2012) and Ward et al. (2016), the only way to observe temperature patterns in cities explicitly and comprehensively is through aerial perspective using thermal remote sensing, which provides LST.

The research conducted by Barros and Lombardo (2016) attested to the efficiency of surface temperature measurements from Landsat 5 Thematic Mapper images in the municipality of São Paulo (SP), Brazil. Thus, thermal satellite images offer great potential for improving the understanding of urban climate dynamics. However, one of the limitations in the approach applied to remote sensing refers to the meticulous acquisition of orbital images, since cloud incidence and spatial resolution can influence the results generated.

In this context, the research gap study examined the problem of UHI in Recife and the correlation of this phenomenon with the temporal variability of land use and land cover, using remote sensing techniques through cloud processing with the JavaScript programming language.

Methodology

Study area

The city of Recife, the capital of the state of Pernambuco, is located in the Northeast region of Brazil, at the coordinates 8º04'03" South latitude and 34º55'00" West longitude (Figure 1). According to data from the Brazilian Institute of Geography and Statistics (IBGE, 2022), Recife has a territorial extension of 218.843 km^2, with an estimated population of 1,653,461 inhabitants and a population density of 7,039.64 inhabitants/km^2 (2020).

Cabral and Alencar (2005) emphasized that Recife has a hot and humid tropical climate, with a plain formed by fluvial-marine sediments and semi-surrounded by hills. The Metropolitan Region of Recife is located in the intertropical zone, with an urban area situated approximately 8° South of the Equator. Due to its location at low latitudes, it presents monthly average temperatures above 25°C, an annual thermal amplitude above 5°C, and an average annual relative humidity of 84% (Mendes et al., 2019).

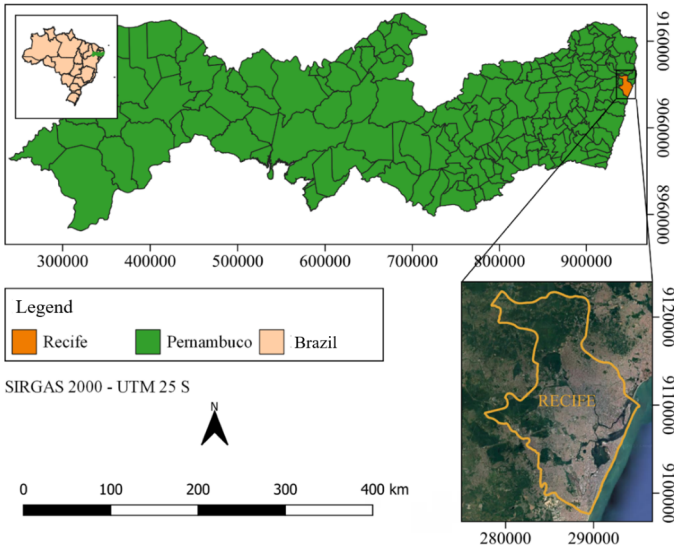

Figure 1 – Location of the study area.
SIRGAS: Geodetic Reference System for the Americas; UTM: Universal Transverse Mercator.

Recife is characterized by being densely urbanized, with most of its extension occupied by buildings and paved streets, except for areas covered by watercourses and small green areas corresponding to parks, squares, and mangroves.

Analysis of rainfall and external ambient temperature

Meteorological data were exported from the National Institute of Meteorology (*Instituto Nacional de Meteorologia* [INMET], 2022) database, obtained from the automatic surface observation meteorological station installed in the Várzea neighborhood of Recife (Recife A301).

This station collects data on external ambient temperature, relative humidity, precipitation, solar radiation, wind direction and speed, and atmospheric pressure. Monthly accumulated precipitation and monthly average temperature data were used for the region's climatic analysis (INMET, 2022). Figure 2 shows the city of Recife's climograph for the years 2013, 2019, and 2021.

Bagyaraj et al. (2023) stated that meteorological factors such as air temperature, precipitation, humidity, and wind speed significantly affect increasing surface temperature, highlighting the importance of understanding the variability of precipitation and temperature in the study area over the years.

It was evident that the months from April to August showed higher precipitation values, characterizing the region's rainy season, and during this period, lower air temperatures were observed. The months from September to February registered the lowest monthly precipitation values, identifying the dry season with higher ambient temperature values.

A trend of higher precipitation values in 2021 was observed compared to the other years. May had the highest recorded precipitation, totaling 533.600 mm, 215.4 mm higher than in 2013 and 312.68 mm higher than in 2019. According to Diem et al. (2024), precipitation patterns can be altered by rising temperatures in cities, modifying atmospheric circulation between urban and rural areas.

The year 2021 revealed the lowest precipitation values during the dry season, with January being the hottest month (27.66°C). In that month, the recorded precipitation was 53.2 mm, 54.4 mm lower than in 2019 and 42.0 mm lower than in 2013 for the same month. The highest temperature during the period was recorded in December 2019 (28.09°C), with precipitation of 88 mm, 165 mm lower than in December 2013.

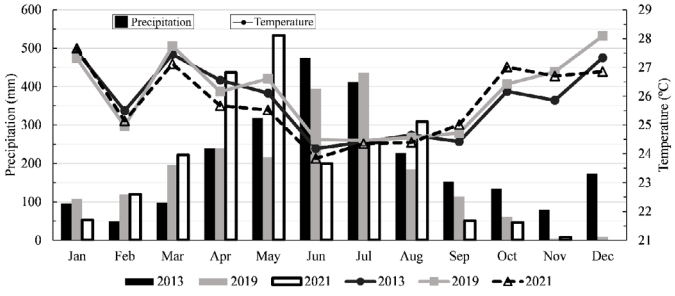

Figure 2 – Climogram of the city of Recife in 2013, 2019, and 2021.

Remote sensing processing

Pre-processing

The acquisition and processing of orbital data were carried out using the Google Earth Engine cloud processing platform's code editor, with the code written in JavaScript. After thoroughly searching available images for the study area, those with the least cloud occurrence were selected. Therefore, images from July 28, 2013 and October 17, 2019, from the Landsat 8 satellite - Operational Land Imager (OLI) sensor (Table 1), and from June 26, 2021, from the Sentinel-2 Multispectral Instrument (MSI) satellite were chosen.

The orbital images and vector files were reprojected to SIRGAS 2000 (Geodetic Reference System for the Americas), Universal Transverse Mercator (UTM) Zone 25 South. After acquiring the images, the processing was performed, considering the clipping of the scene according to the area of interest. For the composition of georeferenced maps with the processed biophysical parameters images—Normalized Difference Vegetation Index (NDVI), Leaf Area Index (LAI), Normalized Difference Built-Up Index (NDBI), Built-Up Index, and LST—the Quantum Geographic Information System (QGIS) software version 2.18.16 and version 3.10 print composition tool was used.

Processing of biophysical parameters

The images obtained from the Landsat 8 OLI were used for processing NDVI, LAI, NDBI, Built-Up Index, and LST, and those obtained from the Sentinel-2 MSI were used for processing NDVI, NDBI, and Built-Up Index because the orbital images exported by MSI do not have a thermal band and, therefore, cannot be applied to surface temperature processing.

The processing of biophysical parameters was carried out with the Google Earth Engine code editor. The Landsat 8 Collection 2 Tier 1 calibrated top-of-atmosphere reflectance and Sentinel-2 MSI Level-1C satellites obtained the corrected planetary reflectance for each band.

Table 1 – Date of the image, time, sun elevation angle, and satellite point.

Satellite Landsat 8 - Operational Lander Imager (OLI)				
Date	**Time (UTM)**	**Sun Elevation Angle**	**Orbit**	**Point**
28/07/2013	12:31:03.60	51.24	214	65
17/10/2019	12:29:27.88	65.97	214	65
Satellite Sentinel 2 - Multispectral Instrument (MSI).				
Date	U.S. Military Grid Reference System			
26/06/2021	25MBM			

Source: Google Earth Engine (2022).
UTM: Universal Transverse Mercator.

The NDVI allows for detecting seasonal and interannual changes in vegetation development and activities, enabling the temporal profile of growth and peak green. It varies between -1 and +1, with values between 0 and 1 for green vegetation surfaces and values below zero for water or clouds (Rouse et al., 1973). NDVI was calculated using Equation 1.

$$NDVI = \frac{\rho_{NIR} - \rho_{RED}}{\rho_{NIR} + \rho_{RED}} \quad (1)$$

Where:
ρ_{NIR} = reflectance of the near-infrared band; and
ρ_{Red} = reflectance of the red band.

The NDBI was developed to identify urban and built-up areas (França et al., 2012). It is based on the increased spectral response of built-up areas between the mid-infrared and near-infrared bands, yielding values between -1 and 1, with positive values corresponding to built-up areas (Zha et al., 2003). NDBI is calculated using Equation 2.

$$NDBI = \frac{\rho_{MIR} - \rho_{NIR}}{\rho_{MIR} + \rho_{NIR}} \quad (2)$$

Where:
ρ_{MIR} = reflectance of the mid-infrared band; and
ρ_{NIR} = reflectance of the near-infrared band.

The Soil-Adjusted Vegetation Index (SAVI) accounts for the effects of exposed soil in the analyzed images (Huete, 1988) and is calculated using Equation 3. The LAI represents the leaf area ratio to the area occupied by that vegetation and serves as an indicator of biomass within a pixel. It was processed according to Allen et al. (2002) using Equation 4. For LAI values lower than 3, the surface emissivity is calculated using Equation 5, also from Allen et al. (2002).

$$SAVI = \frac{(1 + L) * (\rho_{NIR} - \rho_{RED})}{L + \rho_{NIR} + \rho_{RED}} \quad (3)$$

$$LAI = - \frac{\ln\left(\frac{0.69 - SAVI}{0.59}\right)}{0.91} \quad (4)$$

$$\varepsilon_{NB} = 0.97 + 0.0033 * LAI \quad (5)$$

Where:
ρ_{NIR} = near-infrared band;
ρ_{Red} = red band;
L = constant for the index;
ln = natural logarithm, or Napierian logarithm; and
ε_{NB} = emissivity.

The constant for the index (L) is often presented in the literature as a value of 0.5. Emissivity (ε_{NB}) represents the surface's behavior for thermal emission in the relatively narrow band of Landsat. Otherwise, the value of ε_{NB} is 0.98. For the conversion of quantized and calibrated digital number (DN) values from the Landsat 8 OLI sensor system to spectral radiance, radiometric coefficients available in the metadata of the images and sensor characteristics information were used, as per Silva et al. (2016). Thus, Equation 6 was applied to calculate the spectral radiance of the thermal band (Band 10).

$$L_\lambda = ML * Q_{cal} + AL \quad (6)$$

Where:
L_λ = spectral radiance of the sensor in watts ($m^2 \cdot sr \cdot \mu m$);
ML = band 10 rescaling multiplier with a value of 3.3420×10^{-4};
AL = band 10 rescaling additive factor with a value of 0.100; and
Q_{cal} = calibrated quantized value per pixel.

The processing of LST was carried out according to Equation 7, using emissivity, which represents surface behavior for thermal emission in the narrow band, spectral radiance, and calibration constants.

$$LST = \frac{K2}{\ln\left(\frac{\varepsilon_{NB} * K1}{L_\lambda} + 1\right)} \quad (7)$$

Where:
LST = corresponds to the effective satellite temperature in Kelvin (K);
K2 = calibration constant 2 with a value of 1321.08 for Landsat 8 OLI;

ε_{NB} = emissivity;
K1 = calibration constant 1 with a value of 774.89 for Landsat 8 OLI; and
L_λ = spectral radiance of the sensor in watts ($m^2 \cdot sr \cdot \mu m$).

Xu (2008) stated that NDBI can be mixed with noise from other land use classes, such as bare soil, due to the close reflectance values to urban areas. Therefore, He et al. (2010) proposed an index that improves the separation of built-up (impermeable) from non-built-up (permeable) areas, called the Built-Up Index. This index highlights impermeable areas and vegetation in urban environments by considering the relationship between NDBI and NDVI (Equation 8).

$$Built\text{-}Up = NDBI - NDVI \quad (8)$$

Land use and land cover

The study area's land use and cover analysis was performed using products from the MapBiomas Project. The project consists of annual land cover maps and uses products from pixel-by-pixel classification of Landsat satellite images. The process is carried out with extensive machine learning algorithms through the Google Earth Engine platform (MapBiomas, 2022).

For processing, shapefiles of Recife municipality were loaded, followed by Google Earth Engine script to download the maps. The MapBiomas Brazil region (collection 7.0), the study area mask polygon, and the application years were selected for analysis. Subsequently, the maps and area tables for land use and cover classes were exported for the processed years. The generated images were exported to QGIS version 3.10 software to create georeferenced analysis maps.

Results and Discussions

Surface temperature is directly influenced by land use and land cover, as noted by Diem et al. (2024). Green spaces are crucial for maintaining the balance between the Earth's surface temperature and atmospheric parameters. Therefore, changes in land use and land cover classes can significantly influence the urban environment (Tariq et al., 2022; Gemeda et al., 2024).

Figure 3 shows the land use and cover analysis in Recife for 2013, 2019, and 2021. These years were selected for analysis due to the availability of cloud-free orbital images of the study area.

It was observed that there was an increase in the area corresponding to the urban class (represented by the red color). In 2013, the area classified as urban was 117.51 km²; by 2019, this value increased to 121.53 km², and in 2021 it reached 122.74 km² (Table 2).

The data demonstrate that the city is undergoing urban expansion and development, consequently increasing impermeable surfaces. Additionally, pasture areas showed a significant reduction, from 4.93 km² in 2013 to 0.29 km² in 2019 and 0.19 km² in 2021. The areas designated for the Sugarcane, Agriculture-Pasture Mosaic, and River, Lake, and Ocean classes also showed reductions over the eight years of study.

The land use and cover analysis showed an increase in areas with higher urban density (impermeable areas) and a reduction in vegetated areas (permeable areas). This reduction was also noted in the NDVI analysis, where a decrease in vegetated areas was observed, with classes ranging from 0.566 to 0.791 in some specific parts of the municipality, especially in the Várzea neighborhood (Southwest region of Recife) (Figure 4).

Table 2 – Land use and cover classes for the study area in 2013, 2019, and 2021.

Class	Area (km²)		
	2013	2019	2021
Pasture	4.93	0.29	0.19
Sugarcane	1.25	1.08	1.01
Agriculture-Pasture Mosaic	38.03	35.25	34.14
Urban Area	117.51	121.53	122.74
River, Lake, and Ocean	8.19	7.46	6.94

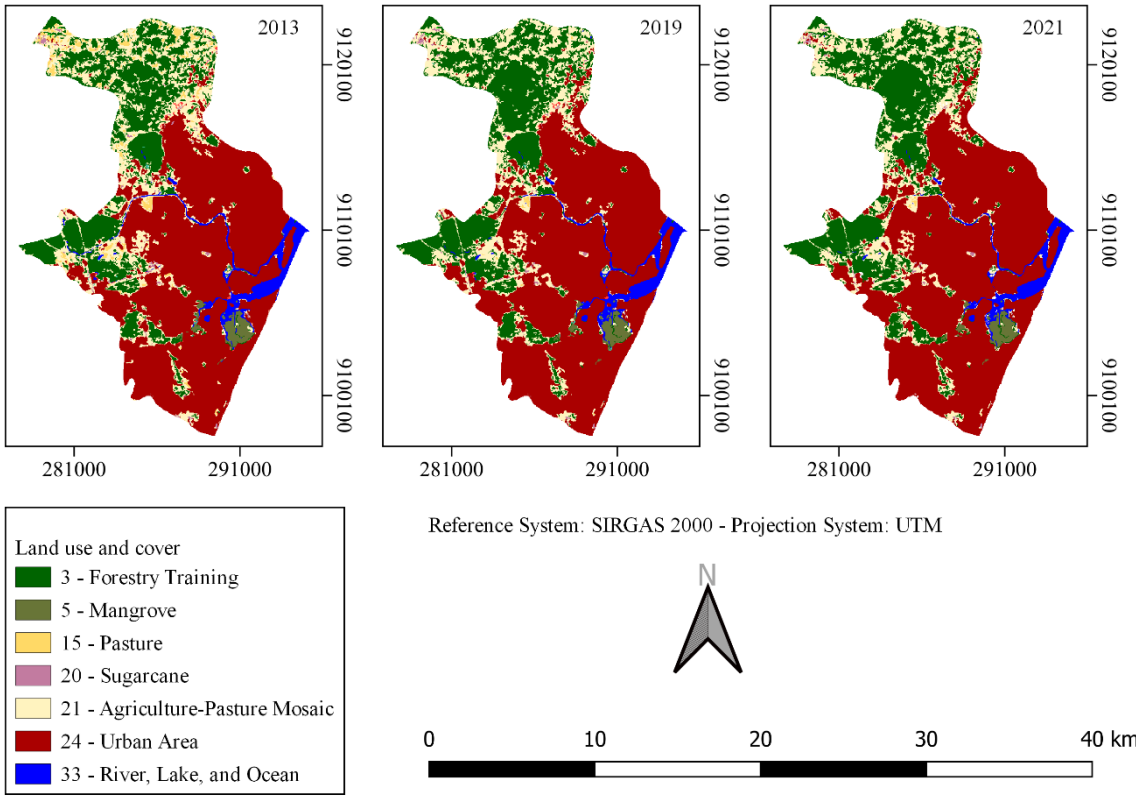

Figure 3 – Land use and cover for 2013, 2019, and 2021.
SIRGAS: Geodetic Reference System for the Americas; UTM: Universal Transverse Mercator.

However, an increase in vegetated areas was noted in the Northern region, indicated by the NDVI.

Still focusing on the NDVI, the statistical data analysis showed that the index value decreased over the years: in 2013, the average NDVI was 0.424; in 2019, it was 0.409; and in 2021, it dropped to 0.385. As shown in Table 3, the maximum NDVI value recorded in the region in 2013 was 0.859, while in 2021, it was 0.851. These values indicate a reduction in the vegetative density of Recife's land cover.

There was an increase in the urban sprawl, located in the Southern part of the city, demarcated by classes with values between 0.115 and 0.341, identified by the orange coloration. According to Borges et al. (2022), the urban climate is determined by built density, which depends mainly on population and urban structure. The increase in urban density in Recife between 2013 and 2021 is evidenced by the reduction in NDVI values in the urban area. In 2021 (Figure 4), the urban sprawl appeared redder than in previous years, revealing the reduction in the index value in that region.

Vegetation is the main source of moisture. The conversion of vegetated areas to developed areas leads to a drastic reduction in humidity. When vegetated areas are converted into developed areas, the excess heat stored in developed areas and the absence of moisture significantly increase the LST (Igun and Williams, 2018; Imran et al., 2019). Bagyaraj et al. (2023) emphasized that the type of land cover significantly influences changes in the urban environment.

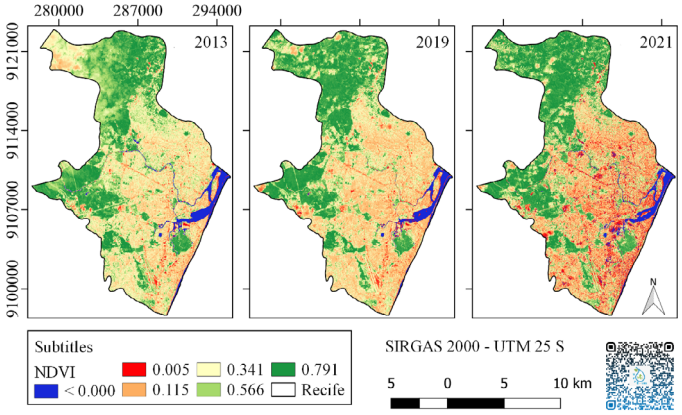

Figure 4 – Normalized Difference Vegetation Index in Recife for 2013, 2019, and 2021.
SIRGAS: Geodetic Reference System for the Americas; UTM: Universal Transverse Mercator.

Table 3 – Statistical values of Normalized Difference Vegetation Index in 2013, 2019, and 2021.

Year	Maximum	Minimum	Average	Standard deviation
2013	0.859	-1.240	0.424	0.259
2019	0.857	-0.589	0.409	0.254
2021	0.851	-0.517	0.385	0.294

The LAI and NDVI identified the presence of vegetated areas in the Northern part of Recife (Figure 5), characterized by higher index values (green coloration). As detailed in Table 4, the maximum LAI value in 2013 was 6.897, while in 2019, it was 4.655.

A reduction in the leaf area of the city was observed, with the LAI results corroborating those of the NDVI, showing a decrease in the index value in 2019 compared to 2013. The urban infrastructure areas were characterized by LAI values lower than 0.166, shown in orange shades.

The major urban expansion in Recife presented NDBI values between 0.033 and 0.204. In 2013, the NDBI showed lighter tones, characterizing lower index values (Figure 6). In 2019 and 2021, the urban area displayed more intense colors due to higher NDBI values, indicating increased urban density over the years. It was noted that 69.44% of Recife's area has a higher urban density, while 30.56% has a higher vegetative density.

The NDBI results were consistent with the NDVI and LAI values. Negative NDBI values (-0.309 to -0.480) were observed in areas with vegetation cover. Studies by Albuquerque et al. (2021) demonstrated that for NDBI, values above 0.400 represent urban areas, exposed impermeable soils, or regions with total vegetation removal. Values between 0.000 and 0.400 represent regions with some type of grass or tree vegetation when performing a comparative analysis of NDVI and NDBI, using CBERS-4 (China-Brazil Earth Resources Satellite) images in central Pará.

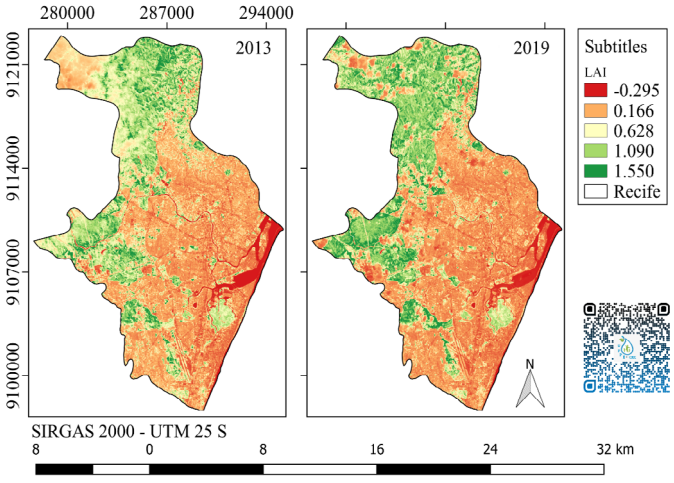

Figure 5 – Leaf Area Index in Recife for 2013 and 2019.
SIRGAS: Geodetic Reference System for the Americas; UTM: Universal Transverse Mercator.

Table 4 – Statistical values of Leaf Area Index in 2013 and 2019.

Year	Maximum	Minimum	Average	Standard deviation
2013	6.897	-0.487	0.477	0.477
2019	4.655	-0.405	0.478	0.531

To improve the analysis of Recife's urban growth, the Built-Up Index was chosen to extract the built surface due to its precision in separating urban areas and exposed soil, as per He et al. (2010).

Studies by Im et al. (2012) and Varshney (2013) demonstrated that the Built-Up Index can separate urban surfaces and provide methods to improve the identification of urban growth. The Built-Up Index's application allows the evaluation of the densification of built-up areas and more accurately defines the boundaries between rural and urban areas.

The Built-Up Index showed values of -0.127 for 2013 in the urban infrastructure area. By 2019, an increase in the index (between -0.127 and 0.247) was observed, characterized by a more intense brown coloration. In 2021, the Built-Up Index reached 0.247, indicating an increase in urban density in the city (Figure 7).

The increase in built-up areas and the reduction in vegetated areas, as evidenced by the analyzed index maps, are key factors contributing to the rise in city temperatures and the occurrence of the heat island phenomenon.

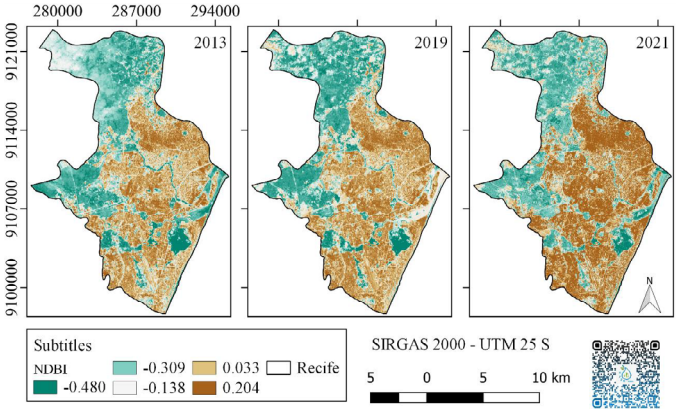

Figure 6 – Normalized Difference Built-Up Index in Recife for 2013, 2019, and 2021.
SIRGAS: Geodetic Reference System for the Americas; UTM: Universal Transverse Mercator.

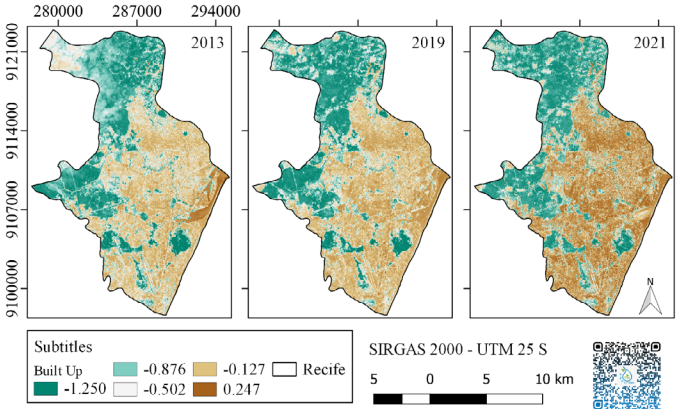

Figure 7 – Built-up in the study area for 2013, 2019, and 2021.
SIRGAS: Geodetic Reference System for the Americas; UTM: Universal Transverse Mercator.

According to Borges et al. (2022), temperatures in urban sprawl are often higher than in surrounding rural areas, as cities consist of a mosaic of areas with higher and lower temperatures, depending on variations in urban land cover.

Gamarra et al. (2014) analyzed surface temperature estimates to identify the urban sprawl of Londrina in Paraná, Brazil, and affirmed that the aforementioned parameter provides support for the correct identification of urban sprawl practically based on physical considerations, corroborating this study.

Mendes et al. (2022) stated that areas with higher densities of tree vegetation (coastal massifs) show lower surface temperatures than densely built-up areas. In 2013, LST values were lower than those observed in 2019. In the region with the highest percentage of urbanization, the recorded LST was 29.35°C for 2013 and 31.95°C for 2019. This difference of 2.60°C, as illustrated in Figure 8, aligns with the climatological data presented in Figure 2, from July to October. The images analyzed in this study were limited to the available dates.

In the Northern part of the city, where a greater presence of vegetation cover was noticed, surface temperatures ranged from 21.65°C to 24.25°C in 2013 and from 24.25°C to 26.75°C in 2019. It was found that in areas with higher urban density, the encountered surface temperature was up to 5.10°C higher than in vegetated areas in 2013, and this value increased to 5.20°C in 2019. The LST analysis highlighted a temperature increase across the entire city region. However, the presence of vegetation is a determining factor for improving the urban microclimate.

Figure 9 details the variation in surface temperature in vegetated areas and urban areas in 2013 and 2019. Following the georeferenced maps, areas with a higher percentage of vegetation showed lower surface temperatures than in more urbanized areas, where temperatures increased.

The analyzed biophysical parameters highlighted the reduction in vegetated areas and the increase in built-up areas over the studied years.

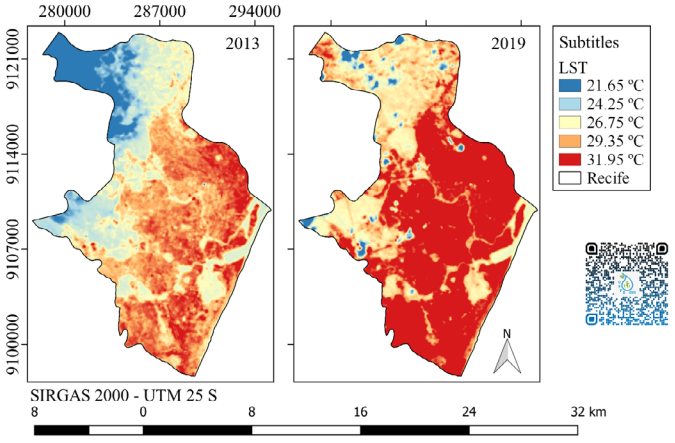

Figure 8 – Land Surface Temperature in the study area for 2013 and 2019.
SIRGAS: Geodetic Reference System for the Americas; UTM: Universal Transverse Mercator.

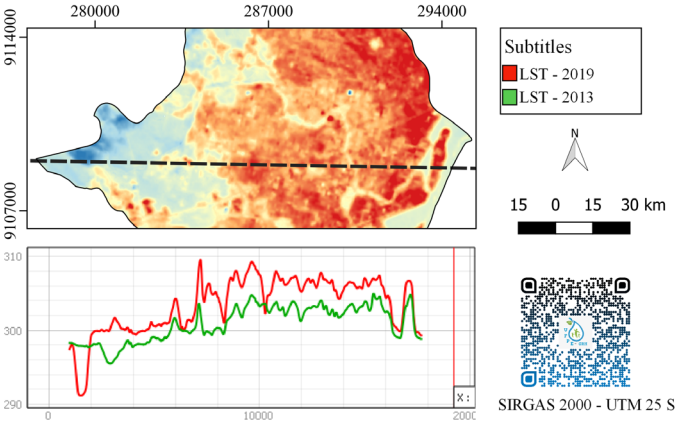

Figure 9 – Land Surface Temperature profile for the years 2013 and 2019. SIRGAS: Geodetic Reference System for the Americas; UTM: Universal Transverse Mercator.

This factor contributed to the increase in surface temperature in 2019 compared to 2013, as shown in the studied profile, thus raising the risk of the occurrence of the heat island phenomenon.

Conclusions

The applicability of biophysical parameters, land use and land cover classification, and LST has proven to be highly effective for understanding and studying the heat island phenomenon in large urban centers. The 2021 data showed that 69.44% of the city of Recife's area has higher urban density.

The land use and cover analysis showed an increase in areas with higher urban density (impermeable areas) and a reduction in vegetated areas (permeable areas), as recorded by MapBiomas data. This reduction is also noted in the NDVI analysis, where the index value decreased over the years: in 2013, the average NDVI value was 0.424; in 2019, it was 0.409; and in 2021, it was 0.385. The LAI and NDVI demonstrate the presence of vegetated areas in the Northern part of Recife.

The major urban expansion of the city showed NDBI values between 0.033 and 0.204, identifying the urban area. Higher NDBI values were recorded in 2019 and 2021, indicating an increase in urban density over the years, a result also evidenced by applying of the Built-Up Index. It was found that in areas with higher urban density, surface temperatures were up to 5.20°C higher than in vegetated areas, in both the 2013 and 2019 images. The results, therefore, demonstrate that there has been an increase in built-up areas in the city. The observed temperature differentiation is due to the different months of the images, requiring further temporal investigation.

Acknowledgments

The authors thank the Foundation for the Support of Science and Technology of Pernambuco (FACEPE) for the doctoral scholarship (IBPG-1657-3.01/21) of the first author, Coordination for the Improvement of Higher Education Personnel (CAPES, *Coordenação de Aperfeiçoamento de Pessoal de Nível Superior*) for the doctoral scholarship (process number: 88887.827976/2023-00) of the second author, the research project "Use of socio-inclusive green technologies as measures for urban drainage control" (process number 408269/2023-5) of the last author, the United States Geological Survey (USGS) for the acquisition of the satellite image, and the National Institute of Meteorology (INMET, *Instituto Nacional de Meteorologia*) for the meteorological data.

Authors' contributions

Leonardo, H.R.A.L.: conceptualization; formal analysis; funding; investigation; methodology; writing – original draft; writing – review & editing. **Almeida**, D.N.O.: formal analysis; funding; validation; visualization; writing – original draft; writing – review & editing. **Amorim**, A.R.: methodology; visualization. **Paiva**, A.L.R.: supervision; writing – review & editing. **Oliveira**, L.M.M.: methodology; project administration; supervision; validation; visualization; writing – original draft; writing – review & editing. **Santos**, S.M.: supervision; validation; visualization; writing – review & editing.

References

Albuquerque, R.S.; Candeia, B.A.; Tavares Júnior, J.R., Candeias, A.L.B., 2021. Comparison of NDVI and NDBI indices for MUX/IRS/CBERS-4 images with digital number (ND) and monochromatic reflectance (ρ). Journal of Hyperspectral Remote Sensing, v. 11 (1), 73-85. https://doi.org/10.29150/2237-2202.2021.250105.

Allen, R.; Bastiaanssen, W.; Waters, R.; Tasumi, M.; Trezza, R., 2002. Surface energy balance algorithms for land. Advance Training and User's Manual. version 1.0. University of Idaho, Kimberly, Idaho, USA, 98 p.

Almeida, C.R.; Teodoro, A.C.; Gonçalves, A., 2021. Study of the urban heat island (UHI) using remote sensing data/techniques: a systematic review. Environments, v. 8 (10), 105. https://doi.org/ 10.3390/environments8100105.

Bagyaraj, T.; Senapathi, V.; Karthikeyan, S.; Chung, S.Y.; Khatibi, R.; Nadiri, A.A.; Lajaver, B.A., 2023. A study of urban heat island effects using remote sensing and GIS techniques in Kancheepuram, Tamil Nadu, India. Urban Climate, v. 51, 101597. https://doi.org/10.1016/j.uclim.2023.101597.

Barros, H.R., Lombardo, M.A., 2016. Urban heat island and land use and land cover in São Paulo-SP. GEOUSP Espaço e Tempo (Online), v. 20 (1), 160-177. https://doi.org/10.11606/issn.2179-0892.geousp.2016.97783.

Borges, V.O.; Nascimento, G.C.; Celuppi, M.C.; Lúcio, P.S.; Tejas, G.T.; Gobo, J.P.A., 2022. Local climate zones and Urban Heat Islands: a systematic review. Revista Brasileira de Climatologia, Dourados, v. 31 (8), 98-127. https://doi.org/10.55761/abclima.v31i18.15755.

Cabral, J.J.S.P.; Alencar, A.V., 2005. Recife e a convivência com as águas. In: Hydroaid (Itália), PMSS/Ministério das Cidades (Org.), Gestão do território e manejo integrado das águas urbanas. Brazil-Italy Cooperation in Environmental Sanitation. Ed. Gráfica Brasil, Ministério das Cidades, Brasília, pp. 111-130.

Cheela, V.R.S.; John, M.; Biswas, W.; Sarker, P., 2021. Combating urban heat island effect — a review of reflective pavements and tree shading strategies. Buildings, v. 11 (13), 93. https://doi.org/10.3390/buildings11030093.

Diem, P.K.; Nguyen, C.T.; Diem, N.K.; Diep, N.T.H.; Thao, P.T.B.; Hong, T.G.; Phan, T.N., 2024. Remote sensing for urban heat island research: Progress, current issues, and perspectives. Remote Sensing Applications: Society and Environment, v. 33, 10108. https://doi.org/10.1016/j.rsase.2023.101081.

França, A.F.; Tavares Júnior, J.R.; Moreira Filho, J.C.C., 2012. Índices NDVI, NDWI e NDBI como ferramentas ao mapeamento temático do entorno da lagoa olho d'água, em Jaboatão dos Guararapes-PE. In: Anais do IV Simpósio Brasileiro de Ciências Geodésicas e Tecnologia da Geoinformação [internet]; 2012 May 06-09; Recife, PE: Departamento de Engenharia Cartográfica da Universidade Federal de Pernambuco – UFPE, pp. 01-09 (Accessed March 15, 2024) at:. https://www3.ufpe.br/cgtg/SIMGEOIV/CD/

Gamarra, N.L.R.; Corrêa, M.D.P.; Targino, A.C.D.L., 2014. Use of remote sensing to retrieve surface albedo and land surface temperature in Londrina (Paraná): a contribution to urban heat island studies. Revista Brasileira de Meteorologia, v. 29 (4), 537-550. https://doi.org/10.1590/0102-778620130671.

Gemeda, D.O.; Kenea, G.; Teshome, B.; Daba, G.L.; Argu, W.; Roba, Z.R., 2024. Impact of land use and land cover change on land surface temperature: Comparative studies in four cities in southwestern Ethiopia. Environmental Challenges, v. 16, 101002. https://doi.org/10.1016/j.envc.2024.101002

Google Earth Engine, 2022. Code editor (Accessed September 25, 2022) at:. https://code.earthengine.google.com/

He, C.; Shi, P.; Xie, D.; Zhao, Y., 2010. Improving the normalized difference built-up index to map urban built-up areas using a semi-automatic segmentation approach. Remote Sensing Letters, v. 1 (4), 213-221. https://doi.org/10.1080/01431161.2010.481681.

Huete, A.R., 1988. Adjusting vegetation indices for soil influences. International Agrophysics, v. 4 (4), 367-376.

Instituto Brasileiro de Geografia e Estatística (IBGE), 2022. Cidades e Estados. Recife (Accessed on June 1, 2022) at:. https://www.ibge.gov.br/cidades-e-estados/pe/recife.html.

Igun, E.; Williams, M., 2018. Impact of urban land cover change on land surface temperature. Global Journal of Environmental Science and Management, v. 4 (1), 47-58. https://doi.org/10.22034/gjesm.2018.04.01.005.

Im, J.; Lu, Z.; Rhee, J.; Quackenbush, L.J., 2012. Impervious surface quantification using a synthesis of artificial immune networks and decision/regression trees from multi-sensor data. Remote Sensing of Environment, v. 117, 102-113. https://doi.org/10.1016/j.rse.2011.06.024.

Imran, H.M.; Kala, J.; Ng, A.W.M.; Muthukumaran, S., 2019. Impacts of future urban expansion on urban heat island effects during heatwave events in the city of Melbourne in southeast Australia. Quarterly Journal of the Royal Meteorological Society, v. 145, 2586-2602. https://doi.org/10.1002/qj.3580.

Instituto Nacional de Meteorologia (INMET), 2022. Dados históricos de pluviometria. (Accessed on November 9, 2022) at: https://portal.inmet.gov.br/dadoshistoricos

MapBiomas, 2022. Coleção MapBiomas (Accessed on October 28, 2022) at: https://mapbiomas.org/colecoes-mapbiomas-1?cama_set_language=pt-BR

Mendes, J.V.; Armond, N.B.; Silva, L.C.B., 2022. Urban Heat Islands, heat waves, and cold waves in the municipality of Rio de Janeiro – RJ (2015-2019). Revista Brasileira de Climatologia, Dourados, v. 30, 133-155. https://doi.org/10.55761/abclima.v30i18.14908.

Mendes, T.G.L.; Anjos, R.S.; Santos, T.N.; Moreira, A.B.; Nóbrega, R.S., 2019. Scientific approach on heat islands in Recife-PE. Journal of Environmental Analysis and Progress, v. 04 (1), 001-013. https://doi.org/10.24221/jeap.4.1.2019.2058.001-013.

Moazzam, M.F.U.; Doh, Y.H.; Lee, B.G., 2022. Impact of urbanization on land surface temperature and surface urban heat island using optical remote sensing data: a case study of Jeju Island, Republic of Korea. Building and Environment, v. 222, 109368. https://doi.org/10.1016/j.buildenv.2022.109368.

Peng, S.; Piao, S.; Ciais, P.; Friedlingstein, P.; Ottle, C.; Bréon, F.M.; Nan, H.; Zhou, L.; Myneni, R.B., 2012. Surface urban heat island across 419 global big cities. Environmental Science & Technology, v. 46 (2), 696-703. https://doi.org/10.1021/es2030438.

Rouse, J.W.; Haas, R.H.; Schell, J.A.; Deering, D.W., 1973. Monitoring Vegetation Systems in the Great Plains with ERTS (Earth Resources Technology Satellite). In: Proceedings of 3rd Earth Resources Technology Satellite Symposium [internet]; 1973 December 10-14, Washington DC, USA: Goddard Space Flight Center. [Paper A20], pp. 309- 317 (Accessed April 10, 2024) at:.https://ntrs.nasa.gov/citations/19740022614

Silva, B.B.; Braga, A.C.; Braga, C.C.; Oliveira, L.M.M.; Montenegro, S.M.G.L.; Barbosa Junior, B., 2016. Procedures for calculation of the albedo with OLI-Landsat 8 images: Application to the Brazilian semi-arid. Revista Brasileira de Engenharia Agrícola e Ambiental, v. 20 (1), 3-8. https://doi.org/10.1590/1807-1929/agriambi.v20n1p3-8.

Tariq, A.; Mumtaz, F.; Zeng, X.; Baloch, M.Y.J.; Moazzam, M.F.U., 2022. Spatio-temporal variation of seasonal heat islands mapping of Pakistan during 2000–2019, using day-time and night-time land surface temperatures MODIS and meteorological stations data. Remote Sensing Applications: Society and Environment, v. 27, 100779. https://doi.org/10.1016/j.rsase.2022.100779.

Varshney, A., 2013. Improved NDBI differencing algorithm for built-up regions change detection from remote-sensing data: an automated approach. Remote Sensing Letters, v. 4 (5), 504-512. https://doi.org/10.1080/2150704X.2013.763297.

Venkatraman, S.; Kandasamy, V.; Rajalakshmi, J.; Sabarunisha, B.S.; Sujatha, M., 2024. Assessment of urban heat island using remote sensing and geospatial application: a case study in São Paulo city, Brazil, South America. Journal of South American Earth Sciences, v. 134, 104763. https://doi.org/10.1016/j.jsames.2023.104763.

Ward, K.; Lauf, S.; Kleinschmit, B.; Endlicher, W., 2016. Heat waves and urban heat islands in Europe: A review of relevant drivers. Science of The Total Environment, v. 569-570, 527-539. https://doi.org/10.1016/j.scitotenv.2016.06.119.

Xu, H., 2008. A new index for delineating built-up land features in satellite imagery. International Journal of Remote Sensing, v. 29 (14), 4269-4276. https://doi.org/10.1080/01431160802039957.

Yin, Z.; Liu, Z.; Liu, X.; Zheng, W.; Yin, L., 2023. Urban heat islands and their effects on thermal comfort in the US: New York and New Jersey. Ecological Indicators, v. 154. https://doi.org/10.1016/j.ecolind.2023.110765.

Zha, Y.; Gao, J.; Ni, S., 2003. Use of normalized difference built-up index in automatically mapping urban areas from TM imagery. International Journal of Remote Sensing, v. 24 (3), 583-594. https://doi.org/10.1080/01431160304987.